Atmospheric pCO_2 sensitivity to the solubility pump: Role of the low-latitude ocean

T. DeVries[1] and F. Primeau[1]

Received 6 April 2009; revised 30 June 2009; accepted 27 July 2009; published 3 November 2009.

[1] Previous research has shown that the atmospheric pCO_2 sensitivity to changes in low-latitude sea-surface chemistry ("low-latitude sensitivity") depends on both the volume of the ocean ventilated from low latitudes and on the degree of air-sea disequilibrium at high latitudes. However, it is not clear which effect is more important. In this paper we present a diagnostic framework for quantifying the relative importance of low-latitude ventilation versus high-latitude air-sea disequilibrium in determining the low-latitude sensitivity of ocean carbon cycle models. The diagnostic uses a Green function that partitions the ocean's carbon inventory on the basis of whether the carbon last interacted with the atmosphere in the low latitudes or in the high latitudes. The diagnostic is applied to a simple 3-box model, a box model with a ventilated thermocline, and a suite of OGCM runs meant to capture a range of possible ocean circulations for present and last-glacial-maximum conditions. The diagnostic shows unambiguously that the OGCM has a greater low-latitude sensitivity than the box models because of the greater amount of water ventilated from low latitudes in the OGCM. However, when applied to the suite of OGCM runs, the diagnostic also reveals that the effect of high-latitude air-sea disequilibrium can sometimes dominate the effect of low-latitude ventilation and is highly sensitive to the state of the ocean circulation. In particular, the magnitude of the high-latitude disequilibrium effect correlates strongly with the strength of the Atlantic meridional overturning circulation and the volume of water ventilated from northern high latitudes.

Citation: DeVries, T., and F. Primeau (2009), Atmospheric pCO_2 sensitivity to the solubility pump: Role of the low-latitude ocean, *Global Biogeochem. Cycles*, *23*, GB4020, doi:10.1029/2009GB003537.

1. Introduction

[2] Ice core records show that during the glacial periods of the past 800,000 years, the partial pressure of atmospheric CO_2 (pCO_2^{atm}) was 80–100 μatm lower than during the corresponding interglacial periods [*Petit et al.*, 1999; *Siegenthaler et al.*, 2005; *Lüthi et al.*, 2008]. By increasing its store of carbon during glacial periods and decreasing it during interglacials, the ocean is believed to have played a dominant role in regulating these pCO_2^{atm} variations (see reviews by *Sigman and Boyle* [2000] and *Archer et al.* [2000a]). Variations in the ocean's carbon inventory are believed to be due to changes in the operation of the ocean's carbon pump [*Volk and Hoffert*, 1985]. The carbon pump is that suite of processes, both physical and biological, that enrich deep ocean waters in dissolved inorganic carbon (DIC) relative to surface waters. With a fixed amount of carbon in the ocean-atmosphere system, and assuming a constant ocean alkalinity, a stronger carbon pump translates to a decrease in the inventory of carbon in the surface ocean and also in the atmosphere which equilibrates with the surface ocean.

[3] Despite decades of research, the exact mechanism whereby the ocean regulates pCO_2^{atm} on glacial-interglacial timescales remains uncertain [see, e.g., *LeGrand and Alverson*, 2001]. One reason for this uncertainty is due to the fact that numerical models disagree on the degree to which changes in the chemistry of the low-latitude surface ocean can alter pCO_2^{atm}. Early box model studies [*Knox and McElroy*, 1984; *Sarmiento and Toggweiler*, 1984; *Siegenthaler and Wenk*, 1984] found that the relatively small area of the cold high-latitude ocean controlled the CO_2 content of the surface low-latitude ocean and of the atmosphere. Later studies pointed out that while pCO_2^{atm} in simple box models is relatively insensitive to changes in low-latitude sea-surface chemistry, three-dimensional dynamical ocean general circulation models (OGCMs) predict a much stronger sensitivity [*Bacastow*, 1996; *Broecker et al.*, 1999]. Low-latitude sensitivity is important because of the large surface area of the low latitude as compared to the high-latitude oceans. As pointed out by *Bacastow* [1996], a strong low-latitude sensitivity implies that changes in the low-latitude sea-surface temperature could contribute significantly to the glacial-interglacial pCO_2^{atm} changes.

[1]Department of Earth System Science, University of California at Irvine, Irvine, California, USA.

0886-6236/09/2009GB003537

[4] Various mechanisms have been proposed to explain the discrepancy between the low-latitude sensitivity of box models and OGCMs. *Archer et al.* [2000b] suggested that diffusive mixing in OGCMs enhanced their low-latitude sensitivity, and showed that a 2-dimensional circulation model could be made to span the range of sensitivities of box models and OGCMs by adjusting the diffusive mixing in the model, with higher diffusivities producing higher low-latitude sensitivities. *Follows et al.* [2002] showed that simple box models were missing important circulation features, resulting in weak low-latitude sensitivities. By adding a box representing the ventilated thermocline to a 3-box model, *Follows et al.* [2002] showed that the sensitivity of the box model could be made to match that of an OGCM. On the other hand, *Toggweiler et al.* [2003] explained the same differences in sensitivity as being due to differences in the degree of air-sea disequilibrium at high-latitude ventilation sites. *Toggweiler et al.* [2003] showed that OGCMs support a greater air-sea disequilibrium than box models, and suggested that this was the ultimate reason for the higher low-latitude sensitivity of OGCMs as compared to box models.

[5] These studies showed that there are two effects that contribute to setting low-latitude sensitivity. The first is the amount of water ventilated from the low latitudes. The second is the degree of air-sea disequilibrium at high-latitude ventilation sites. Distinguishing between the two effects is important because, as pointed out by *Toggweiler et al.* [2003], the former affects nutrient cycling as well, whereas the latter does not, since nutrients do not exchange with the atmosphere. In this way atmospheric pCO_2 sensitivity to the solubility pump can be decoupled from sensitivity to the biological pump. Clearly, a method for quantifying the relative importance of air-sea disequilibrium and the size of the water mass ventilated from low latitudes would help us better understand the role of the low-latitude oceans in regulating atmospheric pCO_2 on glacial-interglacial timescales. In this article we develop a diagnostic formula that allows us to separate and quantify the effects of low-latitude ventilation and high-latitude air-sea disequilibrium on the total low-latitude sensitivity of ocean carbon cycle models.

[6] The key new development which helps us to address the issue of low-latitude sensitivity is the introduction of a Green function which diagnoses the fraction of the ocean volume ventilated from any given patch on the ocean surface. We use the Green function to show that the sensitivity of pCO_2^{atm} to low-latitude solubility perturbations can be expressed as the sum of three terms: (1) a term that is dependent on the volume of the ocean ventilated from low latitudes and independent of air-sea disequilibrium, (2) a term that is dependent on both the volume of the ocean ventilated from high latitudes and the air-sea disequilibrium in high latitudes, and (3) a term that is dependent on the volume of the ocean ventilated from low latitudes and the air-sea disequilibrium in low latitudes. The magnitudes of these three effects can be diagnosed from a perturbation experiment without the need to rerun the model with fast air-sea gas exchange.

[7] The goals of this study are to quantify the magnitudes of the low-latitude ventilation and high-latitude air-sea disequilibrium effects in different types of models, to explore the sensitivity of each effect to the ocean circulation, and to clarify the mechanisms influencing their magnitudes. To make contact with previous work on the issue of low-latitude sensitivity, we revisit the question of why OGCMs are more low-latitude sensitive than box models. We compare the low-latitude sensitivities of the 3-box model of *Toggweiler et al.* [2003], the 5-box model with an explicit thermocline box of *Follows et al.* [2002], and a 3-dimensional abiotic carbon cycling model based on the OGCM of *Primeau* [2005]. Our diagnostic clearly shows that the difference between the low-latitude sensitivities of the three models is due to differences in the amount of water ventilated from the low latitudes.

[8] We also compare the low-latitude sensitivity of several different versions of the OGCM with different surface boundary conditions and different eddy diffusivity parameters. We find that low-latitude sensitivities in this suite of OGCM runs vary by more than a factor of 2, and depend critically on the state of the ocean circulation. Our diagnostic reveals that most of the variability in low-latitude sensitivity is due to variability in the effect of high-latitude air-sea disequilibrium. The disequilibrium effect is strengthened by increasing the strength of the meridional overturning circulation, and by the partitioning of more deepwater ventilation to the North Atlantic. Variability in low-latitude sensitivity is also caused by variability in the amount of water ventilated from low latitudes, which generally increases with higher wind stresses and higher diffusivities, and in the buffering capacity of the ocean, which increases with higher mean ocean temperature and with lower mean ocean pCO_2.

2. Theory

2.1. Factors Influencing Low-Latitude Sensitivity

[9] To illustrate how the sensitivity of pCO_2^{atm} is related to the redistribution of carbon in the ocean-atmosphere system, Figure 1 shows the sense of the carbon flow between the atmospheric, surface, and deep ocean reservoirs as the system adjusts to a cooling perturbation at the surface of the low-latitude ocean. (Following *Bacastow* [1996], *Broecker et al.* [1999], and *Follows et al.* [2002], we use the example of a low-latitude cooling perturbation without taking into account its effect on the ocean circulation to illustrate the sensitivity of the solubility pump to low-latitude perturbations.) A decrease in ocean temperature increases the solubility of CO_2, causing a net flow of carbon from the atmosphere into the low-latitude surface ocean. Subduction and mixing processes transport the surface ocean carbon anomaly into the interior ocean. At the same time, the decreased atmospheric pCO_2 and the increased carbon in the ocean causes an anomalous outgassing of CO_2 at high latitudes. This flow of carbon from the high-latitude ocean to the atmosphere constitutes a negative feedback that tends to decrease the pCO_2^{atm} sensitivity to a low-latitude perturbation. As a result of this redistribution of carbon the system ultimately settles into a new equilibrium state. How

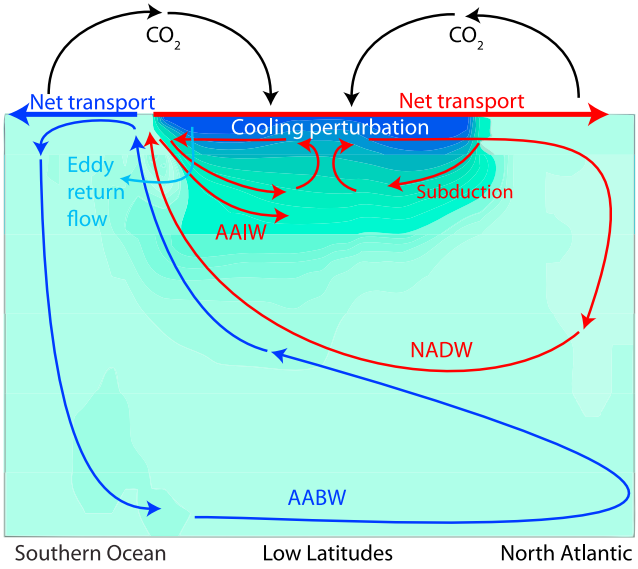

Figure 1. Schematic diagram showing the net flow of carbon between the atmosphere, surface ocean, and deep ocean associated with a cooling of the low-latitude surface ocean. The diagram shows the Atlantic ocean basin since this is where most of the ocean's deep waters form. The general sense of large-scale ocean circulation is redrawn from *Marinov et al.* [2006]. The upper (red) circulation is dominated by a clockwise rotating cell in which low-latitude water flows northward at the surface and is returned southward at depth as North Atlantic Deep Water (NADW). The upper circulation sits on top of the deep (blue) circulation: a counter-clockwise rotating cell with northward flowing Antarctic Bottom Water (AABW) at depth. Antarctic Intermediate Water (AAIW) forms part of the upper ocean circulation as it is entrained into the thermocline. An eddy return flow transports low-latitude waters into the Southern Ocean [*Gnanadesikan*, 1999]. Subduction of mode waters ventilates the thermoclines of the subtropical gyres. In response to the cooling perturbation, CO_2 invades the ocean in the low latitudes. DIC is subducted downward into the thermocline (blue shading) and mixes into the interior ocean. Transport of DIC-enriched surface waters poleward causes anomalous outgassing in the high latitudes. This outgassing represents a negative feedback that tends to damp the atmospheric pCO_2 decrease. How much the atmospheric pCO_2 drops in response to the cooling (i.e., the low-latitude sensitivity) depends on how much of the ocean is ventilated directly from the low latitudes, and on how well the high-latitude surface waters equilibrate with the atmosphere. Low-latitude sensitivity is enhanced by both an increase in the volume of low-latitude waters and by inhibited gas exchange in high-latitude regions.

far this new equilibrium is from the one before the perturbation was applied (i.e., the low-latitude sensitivity) depends on the amount of water that is ventilated directly from low latitudes, and also on the air-sea gas exchange rate and the surface residence time of waters in the high latitudes, which govern how much of the anomalous carbon is released back to the atmosphere.

[10] Both of these effects were originally discussed in a series of papers investigating the reason why OGCMs are more low-latitude sensitive than box models. As suggested by *Broecker et al.* [1999] and *Archer et al.* [2000b], and clearly demonstrated by *Follows et al.* [2002], the low-latitude sensitivity of pCO_2^{atm} depends on the amount of water ventilated from the low-latitude surface ocean. This ventilation can in principle occur through diffusive mixing, as suggested by *Archer et al.* [2000b], but direct measurements of diffusivity in the tropical pycnocline [*Ledwell et al.*, 1993] suggest that this method of ventilation is quite weak. Rather, the formation of a ventilated thermocline in the subtropical gyres, as demonstrated by *Follows et al.* [2002], is the dominant low-latitude mode of ventilation. For the case of a low-latitude cooling, ventilation processes carry the carbon rich surface anomaly into the interior ocean, sequestering carbon in the interior ocean and allowing surface waters to take up more carbon from the atmosphere. On the other hand, *Toggweiler et al.* [2003] highlighted the importance of air-sea disequilibrium in influencing low-latitude sensitivity. High-latitude air-sea disequilibrium increases low-latitude sensitivity because it tends to suppress the outgassing of anomalous carbon at high latitudes, thereby retaining a larger amount of carbon in the ocean.

2.2. Separating the Effects of Low-Latitude Ventilation and Air-Sea Disequilibrium on Low-Latitude Sensitivity

[11] In this section we derive a formula that allows us to quantify the relative impacts of air-sea disequilibrium and low-latitude ventilation on the low-latitude sensitivity of a model. Following *Ito and Follows* [2003], we consider the carbon mass balance for the ocean-atmosphere system, but instead of separating the ocean carbon inventory into upper and deep ocean pools we separate the ocean carbon inventory into high-latitude and low-latitude pools, where by high-latitude pool we mean the carbon that was last in contact with the atmosphere at high latitudes and by low-latitude pool we mean the carbon that was last in contact with the atmosphere at low latitudes. More precisely,

$$C_{total} = M_a pCO_2^{atm} + DIC_L + DIC_H, \quad (1)$$

where M_a is the molar mass of the atmosphere and where DIC_L and DIC_H are the low-latitude and high-latitude dissolved inorganic carbon pools, respectively. Such a decomposition is made possible through the use of the volume integrated Green function $\mathcal{G}(\mathbf{r}_s)$ [e.g., *Primeau*, 2005].

[12] $\mathcal{G}(\mathbf{r}_s)$ can be interpreted as the volume of the ocean per unit surface area, that was last in contact with the atmosphere at the point $\mathbf{r}_s$ on the surface of the ocean. A computationally efficient procedure for computing $\mathcal{G}(\mathbf{r}_s)$ is presented in Text S1, but an intuitive understanding of how to compute it is all that is needed to understand our results.[1] To compute the value of $\mathcal{G}$ for a particular patch of

[1]Auxiliary materials are available with the HTML. doi:10.1029/2009GB003537.

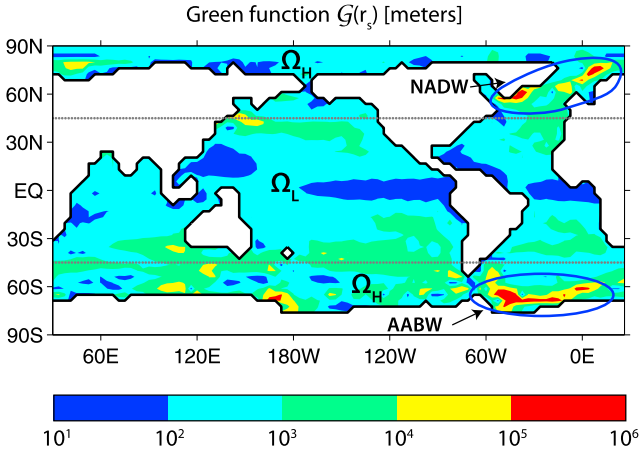

Figure 2. Plot of the Green function $\mathcal{G}(\mathbf{r}_s)$ for OGCM run S1. Note the logarithmic scale. Ω_L is defined on the ocean surface between 45°N and 45°S. Ω_H is defined on the ocean surface outside Ω_L. The plot shows mode waters forming in some areas of the low latitudes, while the major ventilation sites (red) lie in the North Atlantic and Southern Ocean regions. The units of meters result from dividing the volume of the ocean ventilated at each grid point $\mathbf{r}_s$ by the surface area of each grid point.

the surface ocean, one can think of labeling (in a sense, "coloring"), fluid elements as they enter the patch, and removing the color label as soon as a fluid element makes surface contact outside the patch. Taking the whole-ocean inventory, at steady-state, of colored fluid elements labeled in this way, yields the volume of the ocean ventilated through that particular patch. Performing this procedure for every grid point in the model, and dividing by the area of each grid box, yields the full spatial distribution $\mathcal{G}(\mathbf{r}_s)$.

[13] Because $\mathcal{G}(\mathbf{r}_s)$ has units of length, it can also be thought of as an "effective thickness" [*Primeau*, 2005], where the greatest effective thicknesses correspond to places that ventilate the largest part of the interior ocean. The integral of $\mathcal{G}(\mathbf{r}_s)$ over the entire ocean surface Ω gives the total ocean volume,

$$\begin{aligned} \mathrm{V}_{oce} &= \int_{\Omega} \mathcal{G}(\mathbf{r}_s) d^2 r_s \\ &= \underbrace{\int_{\Omega_L} \mathcal{G}(\mathbf{r}_s) d^2 r_s}_{V_L} + \underbrace{\int_{\Omega_H} \mathcal{G}(\mathbf{r}_s) d^2 r_s}_{V_H}, \end{aligned} \tag{2}$$

where in the second line we have partitioned the ocean volume into a volume V_L that was last ventilated through a low-latitude surface patch Ω_L, and a volume V_H that was last ventilated through a high-latitude surface patch Ω_H, with the union of the two regions covering the entire ocean surface. Figure 2 shows a plot of $\mathcal{G}(\mathbf{r}_s)$ for one of the OGCM circulations analyzed in this paper, as well as the regions covered by Ω_L and Ω_H.

[14] The total ocean DIC inventory that cycles through the solubility pump is given by the convolution of $\mathcal{G}(\mathbf{r}_s)$ and the surface DIC field, i.e.,

$$\begin{aligned} \mathrm{DIC}_{oce} &= \int_{\Omega} \mathrm{DIC}(\mathbf{r}_s) \mathcal{G}(\mathbf{r}_s) d^2 r_s, \\ &= \underbrace{\int_{\Omega_L} \mathrm{DIC}(\mathbf{r}_s) \mathcal{G}(\mathbf{r}_s) d^2 r_s}_{DIC_L} + \underbrace{\int_{\Omega_H} \mathrm{DIC}(\mathbf{r}_s) \mathcal{G}(\mathbf{r}_s) d^2 r_s}_{DIC_H}. \end{aligned} \tag{3}$$

[15] To separate the effects of air-sea disequilibrium and low-latitude ventilation on the sensitivity of $p\mathrm{CO}_2^{atm}$ to low-latitude perturbations, we relate the surface ocean DIC concentration to the atmospheric CO_2 content and a local air-sea disequilibrium function,

$$\begin{aligned} \mathrm{DIC}(\mathbf{r}_s) &= F\left(pCO_2^{oce}(\mathbf{r}_s)\right) \\ &= F\left(pCO_2^{atm} - \Delta pCO_2(\mathbf{r}_s)\right) \end{aligned} \tag{4}$$

where $\Delta pCO_2 \equiv p\mathrm{CO}_2^{atm} - pCO_2^{oce}$ is the air-sea disequilibrium function and F represents the equilibrium CO_2 system for seawater. Note that in the limit of infinitely fast air-sea gas exchange $\Delta pCO_2 = 0$ and $p\mathrm{CO}_2^{atm} = pCO_2^{oce}$.

[16] We now consider a perturbation to low-latitude temperature that causes a redistribution of carbon between the atmosphere and ocean. (We should note that while we develop our theory in the context of a temperature perturbation, our results apply equally well to any perturbation to low-latitude sea-surface chemistry. One must simply replace the derivatives with respect to temperature with those with respect to alkalinity, salinity, or DIC.) Taking the derivative of (1) with respect to temperature we obtain

$$M_a \frac{dp\mathrm{CO}_2^{atm}}{dT} + \frac{d\mathrm{DIC}_L}{dT} + \frac{d\mathrm{DIC}_H}{dT} = 0. \tag{5}$$

[17] As already mentioned we neglect the change in the ocean circulation due to the temperature perturbation so that $d\mathcal{G}(\mathbf{r}_s)/dT = 0$. In this case, the derivative of DIC_L with respect to a low-latitude temperature perturbation can be expanded into the following expression

$$\begin{aligned} \frac{d\mathrm{DIC}_L}{dT} &= \int_{\Omega_L} \frac{d\mathrm{DIC}(\mathbf{r}_s)}{dT} \mathcal{G}(\mathbf{r}_s)\, d^2 r_s, \\ &= \int_{\Omega_L} \left[\frac{\partial F}{\partial T} + \frac{\partial F}{\partial pCO_2^{oce}} \left(\frac{dp\mathrm{CO}_2^{atm}}{dT} - \frac{d\Delta pCO_2}{dT} \right) \right] \mathcal{G}\, d^2 r_s, \end{aligned} \tag{6}$$

where in the second line we have dropped the spatial dependencies in $\mathcal{G}$, ΔpCO_2, and F for notational convenience, a convention we retain in the equations that follow. The expression for $d\mathrm{DIC}_H/dT$ is similar, except that the integral is taken over Ω_H,

$$\frac{d\mathrm{DIC}_H}{dT} = \int_{\Omega_H} \left[\frac{\partial F}{\partial T} + \frac{\partial F}{\partial pCO_2^{oce}} \left(\frac{dp\mathrm{CO}_2^{atm}}{dT} - \frac{d\Delta pCO_2}{dT} \right) \right] \mathcal{G}\, d^2 r_s. \tag{7}$$

[18] In the above expressions, the partial derivative of F with respect to T represents the change in DIC, holding pCO_2^{oce} fixed, due to the temperature dependence of the solubility coefficient and of the equilibrium constants in the seawater CO_2 system. The partial derivative of F with respect to pCO_2^{oce} represents the change in DIC, holding temperature fixed, due to the change in the sea-surface partial pressure of CO_2.

[19] Substituting (6) and (7) into (5), solving for $dp\mathrm{CO}_2^{atm}/dT$ and multiplying through by δT (which is 0 on Ω_H since the temperature perturbation is confined to the low latitudes) yields

$$\begin{aligned} M_{oa}\delta pCO_2^{atm} = &-\int_{\Omega_L} \mathcal{G}\frac{\partial F}{\partial T}\delta T d^2 r_s \\ &+\int_{\Omega_H} \mathcal{G}\frac{\partial F}{\partial pCO_2^{oce}}\delta\Delta pCO_2 d^2 r_s \\ &+\int_{\Omega_L} \mathcal{G}\frac{\partial F}{\partial pCO_2^{oce}}\delta\Delta pCO_2 d^2 r_s. \end{aligned} \tag{8}$$

where $M_{oa} \equiv M_a + \int_\Omega \mathcal{G}\,\frac{\partial F}{\partial pCO_2^{oce}} d^2 r_s$.

[20] Equation (8) is a diagnostic that quantifies the effects discussed in section 2.1. The first term on the right-hand side quantifies the direct effect of low-latitude ventilation in carrying the carbon perturbation into the deep ocean. We call this the "low-latitude ventilation effect". This is the effect that *Follows et al.* [2002] showed to be an important factor in determining the greater low-latitude sensitivity of OGCMs as compared to box models. OGCMs ventilate more of the interior ocean through the low latitudes, because of the downward Ekman pumping and the formation of a ventilated thermocline, so that $\mathcal{G}(\mathbf{r}_s)$ is bigger in low latitudes and thus for a given temperature change there is a larger perturbation in $p\mathrm{CO}_2^{atm}$. The second term on the right-hand side quantifies how high-latitude ventilation interacts with the air-sea disequilibrium in high latitudes to affect $p\mathrm{CO}_2^{atm}$. It captures the effect that *Toggweiler et al.* [2003] had in mind when they suggested that differences in the high-latitude air-sea disequilibrium between box models and OGCMs could explain their different low-latitude sensitivities. The greater the high-latitude air-sea disequilibrium, the more important this effect becomes. The last term on the right-hand side quantifies how low-latitude ventilation interacts with the air-sea disequilibrium in low latitudes to affect $p\mathrm{CO}_2^{atm}$. This term is generally small enough to be negligible. Note that with infinitely fast air-sea gas exchange both ΔpCO_2 and $d\Delta pCO_2/dT$ vanish so that the last two terms cannot contribute to low-latitude sensitivity.

[21] M_{oa} measures the total inertia of the ocean-atmosphere system, and is closely tied to the buffering capacity of the ocean. M_{oa} can be related to the total "buffered carbon" inventory of the ocean-atmosphere system, defined by *Goodwin et al.* [2007, 2008] as

$$I_B = M_a pCO_2^{atm} + V\frac{\overline{\mathrm{DIC}}}{R_{global}}, \tag{9}$$

where $\overline{DIC}$ is the globally averaged DIC concentration and R_{global} is the globally averaged Revelle buffer factor defined [*Goodwin et al.*, 2007]

$$R_{global} = \frac{\partial pCO_2}{\partial \overline{\mathrm{DIC}}}\frac{\overline{\mathrm{DIC}}}{pCO_2^{atm}}. \tag{10}$$

Combining (9) and (10) and using the fact that

$$\int_\Omega \mathcal{G}\frac{\partial F}{\partial pCO_2} d^2 r_s \equiv V\frac{\partial \overline{\mathrm{DIC}}}{\partial pCO_2}, \tag{11}$$

we obtain the relation

$$M_{oa} = \frac{I_B}{pCO_2^{atm}}. \tag{12}$$

M_{oa} can also be thought of as an inverse sensitivity, where sensitivity S measures the change in atmospheric $p\mathrm{CO}_2$ due to a change in the (nonbuffered) ocean carbon inventory [*Marinov et al.*, 2008b],

$$S = \frac{\delta pCO_2^{atm}}{\delta \mathrm{DIC}_{oce}} \equiv M_{oa}^{-1}. \tag{13}$$

[22] The relationships (12) and (13) show that sensitivity is directly proportional to $p\mathrm{CO}_2$, as shown by *Marinov et al.* [2008b, 2008a], and inversely proportional to the buffered carbon inventory I_B, as shown by *Goodwin et al.* [2009].

[23] In section 3 we will introduce the models used in this study. For each model we will use the diagnostic formula (8) to determine the relative contribution of low-latitude ventilation and high-latitude air-sea disequilibrium to the total low-latitude sensitivity of the model.

3. Models and Methods

3.1. Model Design

[24] For the 3-box model calculations we use the so-called "Harvardton Bear" model [*Bacastow*, 1996; *Knox and McElroy*, 1984; *Sarmiento and Toggweiler*, 1984; *Siegenthaler and Wenk*, 1984]. It consists of three ocean boxes coupled to a well-mixed atmospheric box (Figure 3a). Model parameters not given in the caption to Figure 3 are the same as those used by *Toggweiler et al.* [2003]. No biology is included in the model.

[25] For the 5-box model calculations we used the thermocline box model of *Follows et al.* [2002]. The low-latitude surface ocean is split into two boxes representing the tropical and subtropical ocean (Figure 3b). The interior ocean is partitioned into a deep box and thermocline box, with the thermocline box ventilated through the subtropical ocean.

[26] For the OGCM calculations we use the same circulation model used by *Primeau* [2005], *Primeau and Holzer* [2006], and *Kwon and Primeau* [2006, 2008], coupled to a well-mixed atmospheric box. The ocean model uses the time-averaged flow field from a coarse-resolution three-dimensional dynamical ocean circulation model forced

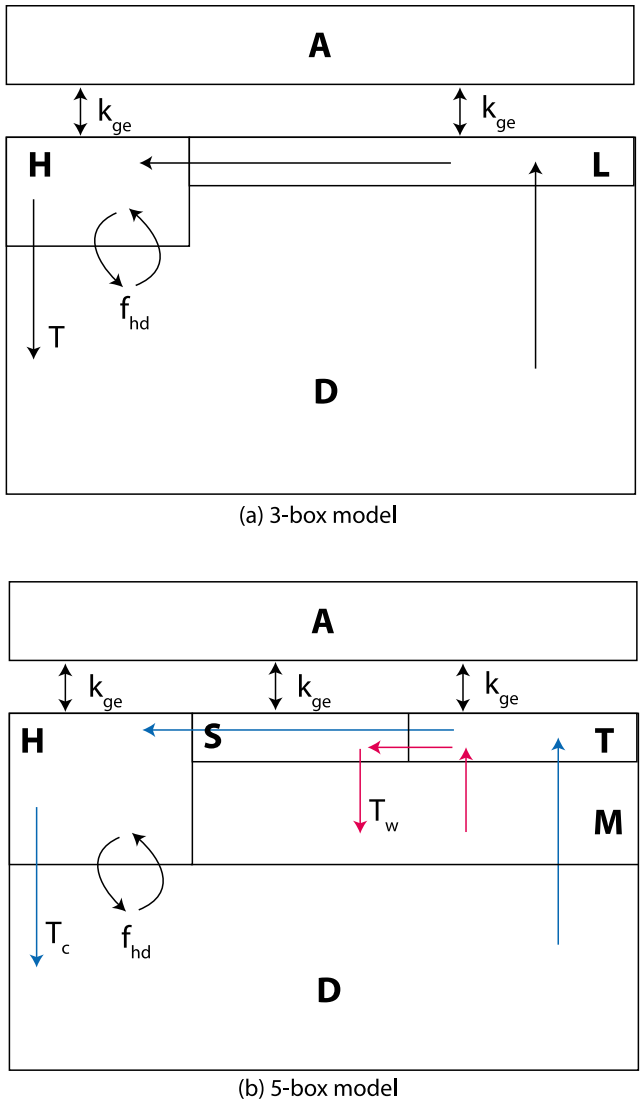

Figure 3. Box model configurations. (a) The 3-box model consists of three ocean boxes H, L, and D, representing the high-latitude, low-latitude, and deep oceans, respectively, coupled to an atmospheric box A. The overturning circulation T is set to 20 Sv, and the high-latitude mixing term f_{hd} is set to 60 Sv. The gas exchange coefficient k_{ge} for the H and L boxes is proportional to the CO_2 solubility and surface area with a piston velocity of 5.5×10^{-5} m/s. Box H has a depth of 250 m and covers 15% of the sea surface, while box L has a depth of 100 m and covers 85% of the sea surface. (b) The 5-box model is modified from the 3-box model to include both tropical (T) and subtropical (S) surface ocean boxes. The cold (blue) overturning T_c is set to 20 Sv, while the warm (red) overturning T_w, which ventilates the thermocline, is set to 5 Sv. The thickness of box H is 1000 m, and the thickness of the thermocline box (M) is 900 m. Box T has a temperature of 25°C and box S has a temperature of 17°C. Boxes S and T each cover 42.5% of the ocean surface area. All other model parameters are the same as in the 3-box model.

with seasonally varying climatological winds, sea-surface temperatures, and sea-surface salinities, as described by *Primeau* [2005]. The equilibrium solution to the abiotic OGCM was found using Newton's method as described by *Kwon and Primeau* [2006].

[27] We also obtained 12 new circulations with our OGCM by restoring the model to different sea-surface temperature and salinity climatologies, and by using different zonal wind stress forcings and different background diffusivities. Each model was spun up for 3000 years and the steady-state advective-diffusive flow was extracted as described by *Primeau* [2005]. The different combinations of surface boundary conditions and diffusivities for each run are described in Table 1.

[28] To facilitate comparison among all of the models we made some minor modifications to the original model formulations. First, we used the equilibrium constants for the CO_2 system recommended by *Zeebe and Wolf-Gladrow* [2001] in all models. Second, we did not include virtual fluxes of carbon due to evaporation and precipitation. Third, we used a uniform piston velocity of 5.5×10^{-5} m/s to drive air-sea gas exchange, as by *Follows et al.* [2002]. Finally, when computing the ocean pCO_2 we used a uniform salinity of 34.7 psu and a uniform alkalinity of 2341 μmol/kg, following the formula given by *Follows et al.* [1996].

3.2. Sensitivity Experiments

[29] With each model we performed two runs to diagnose the low-latitude sensitivity:

[30] 1. A control run in which the total carbon inventory is adjusted so that pCO_2^{atm} is 278 μatm. The same total carbon inventory was kept for run 2.

[31] 2. A temperature perturbation run in which we simulated a cooling of the low-latitude sea surface by reducing the temperature at which the equilibrium constants of the CO_2 system are computed by 6°C, as by *Bacastow* [1996]. For the 3-box model, the low-latitude sea surface is the interface between box L and the atmosphere. For the 5-box model, the low-latitude sea surface is the interface between boxes T and ST and the atmosphere. For the OGCM, we picked the low-latitude sea-surface to be between 45°S and 45°N, in accord with *Follows et al.* [2002]. In all the runs, the physical transport model was "offline" and did not respond dynamically to the imposed temperature perturbation.

[32] Our metric for determining the low-latitude sensitivity of each model is simply the change in pCO_2^{atm} induced by a change of −6°C in the low-latitude temperature (i.e., the difference in pCO_2^{atm} between runs 1 and 2).

[33] For the experiments in which we compared the box models and the OGCM, we also ran analogues of runs 1 and 2 under conditions of "fast gas exchange". In these runs the air-sea gas exchange piston velocity was increased uniformly so that the pCO_2 of the surface ocean was nowhere more than 1 μatm greater or less than that of the atmosphere, as by *Toggweiler et al.* [2003]. The piston velocity in the box models was increased by 100 times, and that in the OGCM by 500 times, relative to the control run to achieve this condition. The total carbon inventory was kept the same as

Table 1. Boundary Conditions and Parameters Used to Obtain New Circulations in the OGCM[a]

"Modern" Runs								
	Temperature and Salinity		Wind Stress			Vertical Diffusivity K_v		
Run	C	WOA05	C	Cx0.5	Cx2	0.5	0.15	0.85
S1	•		•			•		
WL1	•			•		•		
WH1	•				•	•		
KL1	•		•				•	
KH1	•		•					•
WHKL	•				•		•	
S2		•	•			•		
WL2		•		•		•		
WH2		•			•	•		
KL2		•	•				•	
KH2		•	•					•
"LGM" Runs								
	Temperature and Salinity		Wind Stress			Vertical Diffusivity K_v		
Run	PSN	PSN+1	C	Cx0.5	Cx2	0.5	0.15	0.85
LGM1	•		•			•		
LGM2		•	•			•		

[a]The "Modern" runs simulate a range of circulations using modern temperature and salinity forcing. The control (C) temperature and salinity is the climatology used by *Primeau* [2005], while WOA05 indicates the World Ocean Atlas 2005 objectively analyzed monthly mean sea-surface temperature [*Locarnini et al.*, 2006] and salinity [*Antonov et al.*, 2006] averaged over the top 50 m of the ocean. Perturbations from each of the basic states are obtained by increasing or decreasing the zonal wind stress or the background vertical diffusivity. "LGM" runs present two possible glacial circulation states obtained using the GLAMAP last glacial maximum temperature and salinity reconstructions described by *Paul and Schafer-Neth* [2003]. We used the "core" version of the data set available at ftp://ftp.ncdc.noaa.gov/pub/data/paleo/paleocean/by_contributor/paul2003. PSN+1 adds a 1 psu salinity anomaly in the Weddell Sea as suggested by *Paul and Schafer-Neth* [2003], while PSN omits this anomaly. The units of K_v are cm^2/s.

in runs 1 and 2. The fast gas exchange sensitivities provide a check to ensure that (8) correctly diagnoses the effects of air-sea disequilibrium from runs 1 and 2, without having to run the fast gas exchange models.

[34] As already mentioned, we did not include the dynamical effects of the low-latitude temperature change in our experiments. One reason for ignoring the sensitivity of the ocean circulation to low-latitude temperature perturbations is to obtain consistency with previous studies [*Bacastow*, 1996; *Broecker et al.*, 1999; *Follows et al.*, 2002]. Another reason is that the circulation change induced by a cooling confined to low latitudes would be an ad hoc representation of the true ocean response to surface cooling such as occurred during glacial periods, since the actual cooling is likely to have been applied unevenly across the entire ocean surface, including the high latitudes. Rather than guess the right temperature perturbation to apply in the high-latitude regions in the OGCM, we chose to run the OGCM under the different boundary conditions shown in Table 1 to simulate a range of possible ocean circulation states, and then to compare the low-latitude sensitivities of the different model runs using the procedure described above. These runs give a sense of how changes in ocean circulation can affect the low-latitude sensitivity.

4. Results and Discussion

4.1. Comparison of Box Models and an OGCM

[35] Both the amount of water ventilated from low latitudes [*Follows et al.*, 2002] and the air-sea disequilibrium in high latitudes [*Toggweiler et al.*, 2003] have been implicated in enhancing the low-latitude sensitivity of OGCMs as compared to box models. One of the goals of this study is to present a quantitative assessment of the relative importance of each mechanism. Table 2 shows the low-latitude sensitivity of the box models and our standard OGCM, separated according to equation (8) into a low-latitude ventilation effect, a high-latitude air-sea disequilibrium effect, and a low-latitude disequilibrium effect. The pCO_2^{atm} sensitivity of the OGCM to the low-latitude perturbation is more than twice that of the 3-box model, and about 70% greater than that of the 5-box model. Our diagnostic shows that

Table 2. Change in Atmospheric pCO_2 for the Box Models and OGCM Due to a Temperature Decrease of 6°C in the Low-Latitude Patch[a]

Model	Perturbed Patch	δpCO_2^{atm}	Low-Latitude Ventilation Effect	High-Latitude Disequilibrium Effect	Low-Latitude Disequilibrium Effect
3 Box	Box L	−6.42 (−1.73)	−1.62 (−1.68)	−4.86 (−0.06)	0.06 (0.00)
5 Box	Box S and T	−9.37 (−4.72)	−4.58 (−4.67)	−4.83 (−0.05)	0.04 (0.00)
OGCM	45°S - 45°N	−15.70 (−11.25)	−10.97 (−11.24)	−5.34 (−0.01)	0.60 (0.00)

[a]Also shown are changes in pCO_2^{atm} partitioned according to the change due to the low-latitude ventilation effect and the high-latitude and low-latitude disequilibrium effects. The low-latitude ventilation effect and high-latitude and low-latitude disequilibrium effect quantities correspond to the three terms on the right-hand side of equation (8), divided by the inertia M_{oa}. Values in parentheses are results from the fast gas exchange runs. Units are μatm.

Table 3. As in Table 2, Except for the OGCM Sensitivity Runs[a]

Run	δpCO_2^{atm}	Low-Latitude Ventilation Effect	High-Latitude Disequilibrium Effect	Low-Latitude Disequilibrium Effect
S1	−15.70	−10.97	−5.34	0.60
WL1	−13.56	−10.49	−3.67	0.61
WH1	−19.55	−11.66	−8.57	0.68
KL1	−15.88	−10.05	−6.31	0.48
KH1	−17.05	−11.64	−6.13	0.73
WHKL	−23.37	−12.66	−11.61	0.90
S2	−13.44	−10.14	−3.93	0.64
WL2	−11.30	−9.19	−2.62	0.51
WH2	−17.67	−12.14	−6.61	1.08
KL2	−11.48	−8.92	−3.29	0.72
KH2	−14.90	−11.08	−4.59	0.77
LGM1	−24.66	−10.80	−14.55	0.69
LGM2	−18.73	−11.95	−7.44	0.66

[a]Run S1 is the OGCM analyzed in Table 2. Only results from models with normal gas exchange are shown. All units are μatm.

the low-latitude ventilation effect is much stronger in the OGCM than in either of the box models. The high-latitude disequilibrium effect is slightly greater in the OGCM than in the box models, and the low-latitude disequilibrium effect is nearly negligible in all of the models.

[36] Our results show that the OGCM has a higher low-latitude sensitivity than the box models because the OGCM ventilates more water from low latitudes. This is in accord with *Follows et al.* [2002] who showed that the presence of a ventilated thermocline enhances low-latitude sensitivity. Nevertheless, air-sea disequilibrium is an important contributor to low-latitude sensitivity in all three models. The high-latitude disequilibrium effect accounts for most of the low-latitude sensitivity of the 3-box model, 1/2 the sensitivity of the 5-box model, and more than 1/3 of the sensitivity of the standard OGCM. As we will show in section 4.2, the magnitude of the high-latitude disequilibrium effect is highly sensitive to wind stress forcing, diffusivity, and the partitioning of deep ocean ventilation between northern and southern sources. In fact, the high-latitude disequilibrium effect can be greater than the low-latitude ventilation effect.

[37] Table 2 also shows the low-latitude sensitivity of the fast gas exchange models (numbers in parentheses). In the fast gas exchange runs, the pCO_2 of the surface ocean is nowhere more than 1 μatm different from pCO_2^{atm}, so that there is almost perfect air-sea equilibration. The results are as expected. The air-sea disequilibrium effects approach zero, and only the low-latitude ventilation effect remains. The magnitude of the low-latitude ventilation effect is nearly the same as in the standard sensitivity runs. The slightly larger low-latitude sensitivity in the fast gas exchange models is due to a reduction in the inertia M_{oa} which occurs because of a reduction in the buffered carbon inventory. These results indicate that it is not necessary to run additional experiments with fast gas exchange in order to separate the effects of low-latitude ventilation from those of air-sea disequilibrium. It is sufficient to compute the three terms in equation (8) for the standard sensitivity experiments (runs 1 and 2) in order to know the magnitudes of these effects. For this reason, we will not show results of the fast gas exchange models for the remaining experiments.

4.2. Comparison of OGCM Runs With Different Circulations

[38] The results from section 4.1 show that in a realistic ocean circulation model both the low-latitude ventilation effect and the high-latitude disequilibrium effect play a significant role in determining the ocean's low-latitude sensitivity. It is thus worthwhile to explore what mechanisms might influence the magnitudes of each of these effects in the real ocean, as well as the uncertainty in the magnitudes of each effect. To this end we performed the alternate OGCM runs with the boundary conditions and eddy diffusivity parameters given in Table 1. Each of the runs produces a new circulation and temperature field. We have also included two runs in which last glacial maximum (LGM) temperature and salinity reconstructions from *Paul and Schafer-Neth* [2003] are used as boundary conditions in the model. These runs are not meant to produce definitive versions of the actual ocean circulation at the LGM, but are added to help constrain the uncertainty in low-latitude sensitivities by expressing different circulation regimes that could have occurred during the LGM. In all, the alternate OGCM runs are meant to span a reasonable range of uncertainty in the state of the ocean circulation, so that we can gain a sense of how low-latitude sensitivity depends on the state of the ocean circulation.

[39] Table 3 shows the low-latitude sensitivity of the 13 different versions of our OGCM. The drop in atmospheric pCO_2 following low-latitude cooling ranges from 11.30 μatm in run WL2, to 24.66 μatm in run LGM1. In all runs both the low-latitude ventilation effect and the high-latitude disequilibrium effect contribute significantly to the total low-latitude sensitivity. The low-latitude disequilibrium effect remains negligible and will be ignored in our discussion. Our theory and model results will reveal two simple scaling relationships which show that low-latitude sensitivity depends most critically on three factors: the volume of low-latitude waters, the strength of the meridional overturning circulation, and the volume of northern high-latitude waters.

[40] We first consider what mechanisms influence the magnitude of the low-latitude ventilation effect. Under conditions of complete air-sea CO_2 equilibration, we can

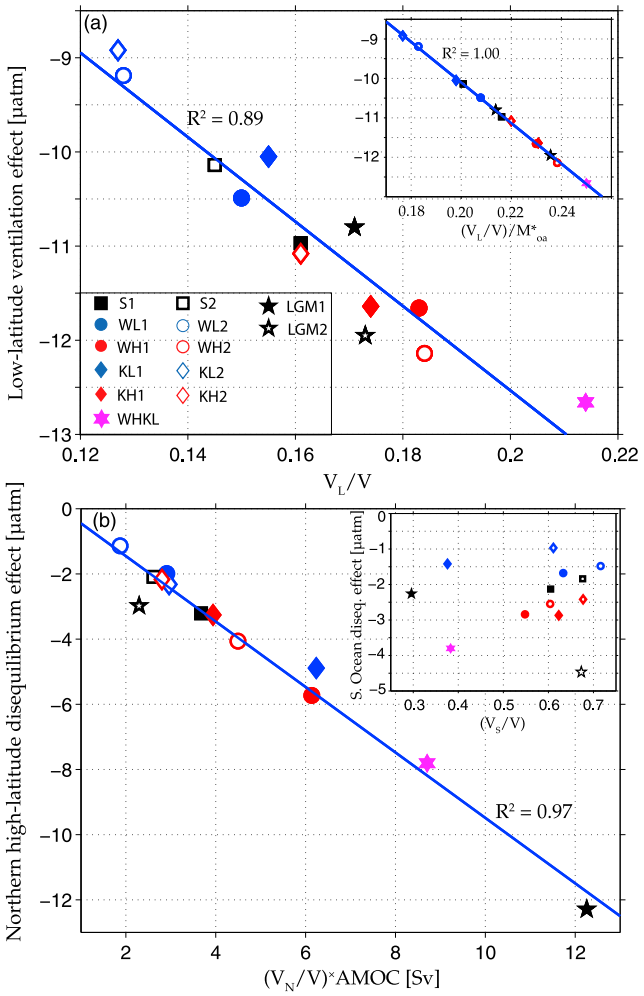

Figure 4. (a) The magnitude of the low-latitude ventilation effect scales linearly with the amount of water ventilated from low latitudes, expressed in this plot as the fraction of the total ocean volume ventilated from low latitudes. Higher low-latitude sensitivities are associated with larger volumes of low-latitude water. The scatter in the plot is due to the fact that the inertia M_{oa}, which depends on the buffering capacity of the ocean, is not constant across all model runs: accounting for this effect eliminates the scatter (inset plot). (b) The magnitude of the air-sea disequilibrium effect in the northern high latitudes scales linearly with the product of the strength of the Atlantic meridional overturning circulation (AMOC) and the fraction of the ocean ventilated from the northern high latitudes, in agreement with the relationship (19) derived in section 4.2 and Appendix A. The magnitude of the disequilibrium effect in the Southern Ocean is generally smaller and less variable in our OGCM runs than that in the northern high latitudes (inset plot).

write the atmospheric pCO_2 sensitivity to a low-latitude temperature perturbation as

$$\delta pCO_2^{atm}|_{vent} = -M_{oa}^{-1} \int_{\Omega_L} \mathcal{G} \frac{\partial F}{\partial T} \delta T d^2 r_s, \qquad (14)$$

which is simply the first term in (8). From (14) we see that if the state of the CO_2 system chemical equilibria is approximately constant across all the models (i.e., M_{oa} and dF/dT are approximately the same), then to a good approximation the magnitude of the low-latitude ventilation effect should scale directly with the volume V_L of water ventilated from low latitudes, since

$$\delta pCO_2^{atm}|_{vent} \propto \int_{\Omega_L} \mathcal{G} d^2 r_s \equiv V_L. \qquad (15)$$

[41] This is precisely the relationship intuited by *Broecker et al.* [1999] and shown clearly in the model comparison study of *Follows et al.* [2002].

[42] Figure 4a shows that the magnitude of the low-latitude ventilation effect does scale linearly with the volume of the ocean ventilated from low latitudes. The scatter in the plot is due to variations in the inertia M_{oa} (Table 4), which depends on the buffering capacity of the ocean. Accounting for this effect by dividing V_L by M_{oa} eliminates the scatter, as shown in the inset plot in Figure 4a. (A perfect correlation is guaranteed by (14) as long as $\partial F/\partial T$ is the same in all runs.) Since the initial atmospheric pCO_2 was kept at 278 μatm for all runs, (12) shows that variations in M_{oa} are due to variations in the buffered carbon inventory. The buffered carbon inventory is sensitive to the ocean circulation through the influence of the ocean circulation on the mean ocean chemistry. In general the buffered carbon inventory increases with higher mean ocean temperature and with lower mean ocean CO_2 concentration.

[43] Our results show that the magnitude of the low-latitude ventilation effect is relatively constant across a wide range of ocean circulations. Figure 4a shows that increasing the background vertical diffusivity or the surface wind stress (red symbols) from the standard cases (S1 and S2) both increase the volume of low-latitude water and enhance low-latitude sensitivity, while decreasing either of these two factors (blue symbols) reduces low-latitude sensitivity. On the other hand, reducing vertical diffusivity in a high wind stress regime increases the volume of low-latitude waters (run WHKL). However, the differences are relatively small in all cases. From these results it appears that the magnitude of the low-latitude ventilation effect is well constrained, and that the solubility effects of low-latitude cooling cannot explain a significant portion of the glacial-interglacial pCO_2^{atm} variability without taking into account the effect of high-latitude air-sea disequilibrium.

[44] The high-latitude air-sea disequilibrium effect is generally smaller than the low-latitude ventilation effect in our runs, but there is more variability across our suite of runs implying a greater uncertainty about its importance in explaining glacial-interglacial pCO_2^{atm} variability. Ignoring the low-latitude ventilation and disequilibrium terms, we can write the atmospheric pCO_2 sensitivity to a low-latitude temperature perturbation as

$$\delta pCO_2^{atm}|_{diseq} = M_{oa}^{-1} \int_{\Omega_H} \mathcal{G} \frac{\partial F}{\partial pCO_2^{oce}} \delta \Delta pCO_2 d^2 r_s, \qquad (16)$$

Table 4. Quantities That Are Relevant to the Low-Latitude Sensitivity for the OGCM Runs[a]

Run	δpCO_2^{atm} (μatm)	V_L/V (unitless)	V_N/V (unitless)	AMOC (Sv)	M^*_{oa} (unitless)
S1	−15.70	0.161	0.234	15.7	0.745
WL1	−13.56	0.150	0.217	13.4	0.722
WH1	−19.55	0.183	0.269	22.8	0.796
KL1	−15.88	0.155	0.469	13.3	0.783
KH1	−17.05	0.174	0.203	19.4	0.754
WHKL	−23.37	0.214	0.403	21.6	0.856
S2	−13.44	0.145	0.179	14.6	0.722
WL2	−11.30	0.128	0.156	12.0	0.700
WH2	−17.67	0.184	0.212	21.2	0.772
KL2	−11.48	0.127	0.262	11.3	0.719
KH2	−14.90	0.161	0.162	17.3	0.732
LGM1	−24.66	0.171	0.533	23.0	0.800
LGM2	−18.73	0.173	0.154	14.9	0.734

[a] V_L is the volume of the ocean ventilated from low latitudes (45°S–45°N), and V_N is the volume of the ocean ventilated from the northern high latitudes (north of 45°N). V is the total ocean volume. AMOC is the maximum strength of the Atlantic meridional overturning circulation north of 45°S. M^*_{oa} is a unitless inertia defined $M^*_{oa} \equiv M_{oa}/(M_a + f_0 \int \mathcal{G} d^2 r_s)$, where f_0 = 1024.5 mol/m^3.

which is just the second term on the right-hand side of (8). Assuming that the state of the CO_2 system equilibria is approximately constant across all runs (i.e., M_{oa} and $\partial F/\partial pCO_2$ are constant), then differences in the high-latitude disequilibrium effect across the runs should scale with the volume of water ventilated from the high latitudes and the disequilibrium anomaly in high latitudes produced by the low-latitude cooling,

$$\delta pCO_2^{atm}|_{diseq} \propto \int_{\Omega_H} \mathcal{G} \delta \Delta pCO_2 d^2 r_s. \tag{17}$$

[45] To rid (17) of the convolution integral, we make the simplifying assumption that the disequilibrium anomaly is uniform at both the northern and southern high-latitude ventilation sites. Under these conditions, (17) reduces to

$$\delta pCO_2^{atm}|_{diseq} \propto V_S \delta \Delta pCO_{2_S} + V_N \delta \Delta pCO_{2_N} \tag{18}$$

where V_S and V_N are the volumes of water ventilated from the southern and northern high latitudes, respectively.

[46] Equation (18) shows that the magnitude of the high-latitude disequilibrium effect is influenced by the magnitude of the disequilibrium anomalies in the southern and northern high latitudes, as well as the partitioning of deep ocean ventilation between southern and northern sources. Our results show that disequilibrium driven through the northern high latitudes is generally larger than that driven through the Southern Ocean, and is also more sensitive to the state of the ocean circulation. For this reason we will focus on mechanisms influencing the disequilibrium anomaly in the northern high latitudes.

[47] In the Atlantic Ocean, the meridional overturning circulation (AMOC) transports low-latitude water northward where it is transformed into NADW (Figure 1). It is intuitively clear that speeding up the AMOC enhances air-sea disequilibrium in the high latitudes by reducing the surface residence time of poleward flowing water parcels. Slowing down the AMOC has the opposite effect. Although the exact relationship between the strength of the AMOC and the air-sea disequilibrium in high latitudes is complicated by diffusive mixing, we show in Appendix A that for purely advective flow and relatively small perturbations to the MOC strength, $\delta \Delta pCO_2$ scales linearly with the strength of the AMOC. The linear relationship holds as long as the surface residence time is long compared to the air-sea equilibration timescale (see equation (A10)). If these conditions are met, then we can use (18) to write

$$\delta pCO_2^{atm}|^N_{diseq} \propto V_N \mathrm{AMOC} \tag{19}$$

where we have focussed only on the component of disequilibrium driven through the northern high latitudes, as indicated by the N superscript.

[48] Figure 4b shows that the relationship (19) holds remarkably well in our OGCM. In the main plot we have shown only that portion of the high-latitude disequilibrium effect that is due to ventilation from areas north of 45°N (obtained by evaluating the integral (16) on Ω_H north of 45°N). The disequilibrium effect is highly sensitive to the state of the ocean circulation through the dependence of the AMOC strength and the volume of northern-source waters on wind stress and vertical diffusivity. Table 4 shows that increasing wind stress in our model both strengthens the AMOC and partitions more ventilation to the north Atlantic, which increases the magnitude of the northern high-latitude disequilibrium effect according to the simple theory (19). Changing the vertical diffusivity κ_v produces two competing effects. On one hand, increasing κ_v increases the strength of the AMOC (Table 4), which tends to increase $\delta pCO_2^{atm}|^N_{diseq}$. This scaling of MOC strength with diffusivity in coarse-resolution OGCMs is a well-known effect [*Bryan*, 1987; *Gnanadesikan*, 1999]. On the other hand, reducing κ_v partitions more of the deep ocean ventilation to the north Atlantic, which also increases the northern high-latitude disequilibrium effect. In most of the runs the two effects nearly cancel, but run KL1 partitions so much more ventilation to the North Atlantic that there is a significant increase (compared to run S1) in the magnitude of the northern high-latitude disequilibrium effect, as well as the high-latitude disequilibrium effect as a whole. When both vertical diffusivity is decreased and wind stress is increased

(run WHKL) the AMOC strengthens, more water is ventilated from the North Atlantic, and the high-latitude disequilibrium effect is enhanced.

[49] The inset plot in Figure 4b shows the weaker and less variable disequilibrium effect that is driven through ventilation in the Southern Ocean, as a function of the fraction of the ocean ventilated south of 45°S. The Southern Ocean disequilibrium effect shows some clear trends if one focusses solely on the effects of changing one parameter. For example increasing wind stress increases the air-sea disequilibrium effect in the Southern Ocean, perhaps due to stronger Ekman pumping associated with stronger westerly winds, while weaker vertical diffusivities reduce the magnitude of the disequilibrium effect in the Southern Ocean by partitioning more ventilation to the north Atlantic. Overall though we could find no clear relationship to explain the variation across all runs. Exchange of low-latitude waters with the Southern Ocean does not follow the simple MOC pattern of the north Atlantic, and is most likely driven by mesoscale eddy transport [*Gnanadesikan*, 1999].

[50] Run LGM1 is a particularly interesting case, because the high-latitude disequilibrium effect is actually larger than the low-latitude ventilation effect. This run highlights the potentially large impact of northern hemisphere air-sea disequilibrium on low-latitude sensitivity. This large impact occurs because the circulation state of LGM1 produces relatively rapid overturning circulation and large volumes NADW. The low-latitude ventilation effect in run LGM1 is comparable in magnitude to the rest of the runs. This emphasizes the point that the low-latitude ventilation effect and the high-latitude disequilibrium effect are two separate effects which are not necessarily correlated.

5. Summary and Conclusions

[51] In this article we developed a diagnostic formula to quantitatively assess the relative importance of both low-latitude ventilation and high-latitude air-sea disequilibrium in setting the low-latitude sensitivity of abiotic ocean carbon cycle models. We applied the formula to sensitivity experiments in which we simulated cooling of the low-latitude surface ocean in two box models and a suite of OGCMs. Our goals were to quantify the magnitudes of the low-latitude ventilation and high-latitude air-sea disequilibrium effects, to explore the sensitivity of each effect to different ocean circulations, and to clarify the mechanisms influencing the magnitude of each effect.

[52] Our main theoretical result is summarized by equation (8), which in conjunction with our experiments tells us the following:

[53] 1. In the limit of infinitely fast gas exchange (i.e., $\Delta pCO_2 = 0$), low-latitude sensitivity depends directly on the volume V_L of the ocean ventilated from low latitudes, that is, on the value of $\mathcal{G}$ on Ω_L. As shown clearly by *Follows et al.* [2002], low-latitude sensitivity is weaker in simple box models without a representation of the ventilated thermocline than in OGCMs. Our diagnostic confirms that the weak low-latitude sensitivity of simple box models is due to the smaller volume of low-latitude water in box models compared to OGCMs, rather than to differences in high-latitude air-sea disequilibrium. A suite of experiments with a coarse-resolution OGCM further confirms the direct correlation between the amount of water V_L ventilated from low latitudes and the low-latitude sensitivity. Increasing the background vertical diffusivity or the surface wind stress from their basic states, increases V_L and enhances low-latitude sensitivity. Small deviations from a direct correlation between V_L and low-latitude sensitivity are found to be due to variations in the buffering capacity of the ocean across model runs.

[54] 2. For finite gas exchange, air-sea disequilibrium in the high latitudes increases low-latitude sensitivity, as suggested by *Toggweiler et al.* [2003]. The magnitude of this "high-latitude disequilibrium effect" depends directly on the degree of high-latitude air-sea disequilibrium and on the volume of the ocean ventilated from high latitudes. Models in which air-sea gas exchange is restricted in the high latitudes where deep waters form will have large low-latitude sensitivities, as claimed by *Toggweiler et al.* [2003]. Our suite of OGCM experiments shows that the magnitude of the high-latitude disequilibrium effect is highly sensitive to the state of the ocean circulation and can approach or exceed that of the low-latitude ventilation effect. Much of the variation in the disequilibrium effect across our suite of OGCM runs can be explained by considering flow from the low latitudes to the high latitudes to be purely advective. This leads to a model which predicts that the magnitude of the high-latitude disequilibrium effect scales directly with the strength of the meridional overturning circulation (MOC). We showed that this relationship holds very well for the water masses forming in the northern high latitudes. Variations in surface wind stress and vertical diffusivity produce highly variable low-latitude sensitivities by varying the MOC strength and by modifying the partitioning of deep ocean ventilation between southern and northern sources.

[55] On the whole, our results do not support a very large role for low-latitude solubility perturbations in explaining glacial-interglacial pCO_2^{atm} variations. Based on the experiments presented in this paper, we believe that the part of the low-latitude sensitivity which is driven by direct ventilation of the interior ocean from the low latitudes is fairly well constrained, and probably not a significant source of glacial-interglacial pCO_2^{atm} variability. However, we have identified some intriguing uncertainty in the degree to which high-latitude disequilibrium can affect the low-latitude sensitivity. Under conditions of rapid meridional overturning and large volumes of water ventilating from the North Atlantic, low-latitude sensitivity can be significantly enhanced. The effect may be even greater with extensive sea ice inhibiting gas exchange. The state of the ocean circulation at the LGM remains highly uncertain [*Wunsch*, 2003; *Gebbie and Huybers*, 2006; *Huybers et al.*, 2007]. Because of this, until the LGM ocean circulation can be better constrained we cannot rule out the possibility of low-latitude solubility perturbations contributing in some significant way to the glacial-interglacial pCO_2^{atm} variability.

[56] A final point we would like to make is to caution against applying the results in this paper to the biological pump. For example, it would be untrue to claim that pCO_2^{atm} sensitivity to perturbations to low-latitude biological

productivity is related to the sensitivity to low-latitude solubility perturbations. The diagnostic presented here, and our analysis, is applicable only to the solubility pump. The component critical to the biological pump that we have not included in our framework is the pool of regenerated carbon in the ocean. The physics governing the transport of regenerated carbon are different from those governing the transport of DIC. Therefore, the response of the ocean-atmosphere system to perturbations in the biological pump could be very different from the response to perturbations in the solubility pump. Green functions analogous to the one presented in this paper can be defined for the regenerated carbon transport pathways, allowing for a framework similar to the one presented here to be developed for the biological pump. We plan to address this issue in a future paper.

Appendix A: High-Latitude Air-Sea Disequilibrium Response to a Low-Latitude Solubility Perturbation

[57] In this section we derive an analytic expression for the air-sea disequilibrium in high latitudes, and show how the anomalous air-sea disequilibrium in high latitudes due to a low-latitude temperature perturbation scales with the strength of the meridional overturning circulation. The expressions are derived for a simple 3-box model without mixing, but as shown in section 4.2 the relationships also apply well to results from the OGCM.

[58] Consider the simple case where the ocean surface is divided into two regions: a low-latitude region and a high-latitude region. Advection transports water from the low latitudes to the high latitudes, as in the 3-box model (Figure 3a). At steady-state in the high-latitude region, there exists a distribution of fluid elements with different residence times in that region. The air-sea disequilibrium is given by the mass-weighted integral of the air-sea disequilibrium of all fluid parcels, i.e.,

$$\Delta pCO_2 = \int_0^\infty \mathcal{Q}(\tau)\Delta pCO_2(\tau)d\tau, \tag{A1}$$

where $\mathcal{Q}(\tau)$ is the residence-time PDF and $\Delta pCO_2(\tau)$ is the air-sea disequilibrium of water parcels with residence time τ. $\mathcal{Q}(\tau)$ has the functional form

$$\mathcal{Q}(\tau) = \frac{1}{\tau_c}\exp(-\tau/\tau_c), \tag{A2}$$

where $\tau_c \equiv V/M$ is a mean surface residence time defined by the volume V of the high-latitude box and the strength M of the overturning circulation.

[59] The air-sea disequilibrium as a function of residence time τ can be derived from the differential equation governing the equilibration of DIC between the atmosphere and ocean,

$$\frac{d\mathrm{DIC}}{d\tau} = -\frac{vA\alpha}{V}\left(pCO_2 - pCO_2^{atm}\right) = \kappa\Delta pCO_2 \tag{A3}$$

where v is the piston velocity in m/yr, A is the surface area of the high-latitude region in m^2, α is the solubility of CO_2 in mol/kg/atm, and $\kappa = vA\alpha/V$. Since DIC is a function of pCO_2 we can write

$$\frac{d\mathrm{DIC}}{d\tau} = \frac{\partial \mathrm{DIC}}{\partial pCO_2}\frac{dpCO_2}{d\tau}, \tag{A4}$$

and substitute this equation into (A3) and integrate to obtain

$$\Delta pCO_2(\tau) = \Delta pCO_{2_0}\exp\left(-\tau/\tau_g\right) \tag{A5}$$

where $\tau_g \equiv (1/\kappa)(\partial DIC/\partial pCO_2)$ is the gas exchange timescale.

[60] Combining (A1), (A2), and (A5) yields,

$$\Delta pCO_2 = \frac{\Delta pCO_{2_0}}{\tau_c}\int_0^\infty \exp\left[-\tau\left(1/\tau_c + 1/\tau_g\right)\right]d\tau, \tag{A6}$$

which can be integrated to obtain an expression for the steady-state air-sea disequilibrium as a function of the initial disequilibrium and two timescales: the gas exchange timescale and the surface residence timescale,

$$\Delta pCO_2 = \Delta pCO_{2_0}\frac{\tau_g}{\tau_c + \tau_g}. \tag{A7}$$

[61] The initial air-sea disequilibrium in the high latitudes depends on the air-sea disequilibrium in the low latitudes as well as the temperature gradient between the low-latitude and high-latitude surface oceans, i.e.,

$$\Delta pCO_{2_0} = \Delta pCO_2^L + \frac{\partial pCO_2}{\partial T}\left(T^L - T^H\right). \tag{A8}$$

[62] Assuming nonlinearities in the CO_2 system equilibrium are small enough so that τ_g is the same both before and after the low-latitude temperature perturbation δT^L, the change in the high-latitude air-sea disequilibrium is given by

$$\delta\Delta pCO_2 \approx \left(\delta\Delta pCO_2^L + \frac{\partial pCO_2}{\partial T}\delta T^L\right)\frac{\tau_g}{\tau_c + \tau_g}. \tag{A9}$$

[63] In the experiments that we performed the magnitude of the temperature perturbation δT^L was a constant 6°C. Additionally, the air-sea disequilibrium in the low latitudes is always small so that to a good approximation $\delta\Delta pCO_2^L$ is a constant. Thus the change in the high-latitude air-sea disequilibrium is proportional to the ratio of the gas exchange and surface residence timescales,

$$\delta\Delta pCO_2 \simeq K\frac{\tau_g}{\tau_c + \tau_g}, \tag{A10}$$

where the constant K is negative for a negative temperature perturbation in the low latitudes.

[64] Equation (A10) predicts that the change in high-latitude air-sea disequilibrium after a perturbation to low-latitude temperature should be sensitive to the surface residence timescale τ_c, which depends on the strength of the meridional overturning circulation M. The sensitivity of

$\delta\Delta pCO_2$ to a change in M can be estimated by expanding (A10) in a Taylor series about a reference value M_0.

$$\delta\Delta pCO_2 = K\left[\frac{\tau_g V\delta M}{\left(V+\tau_g M_0\right)^2} - \frac{\tau_g^2 V\delta M^2}{\left(V+\tau_g M_0\right)^3}\right] + \ldots \quad \text{(A11)}$$

The second-order term can be ignored as long as

$$\left|\frac{\delta M}{M_0}\right| \ll \frac{\tau_{c_0}}{\tau_g} + 1, \quad \text{(A12)}$$

where τ_{c_0} is the reference mean surface residence time corresponding to M_0. Under these conditions $\delta\Delta pCO_2$ scales linearly with a change in the strength of the meridional overturning circulation M.

[65] **Acknowledgments.** T.D. would like to thank the members of his Ph.D. thesis advisory committee: Ellen Druffel, Keith Moore, and John Southon. The authors would also like to thank Eun-Young Kwon for making the code for the implicit ocean biogeochemistry model available. Finally, we would like to thank the two anonymous reviewers for their constructive comments. This research was funded by the National Science Foundation grants OCE 0726871 and OCE 0623647.

References

Antonov, J. I., R. A. Locarnini, T. P. Boyer, A. V. Mishonov, and H. E. Garcia (2006), *World Ocean Atlas 2005*, vol. 2, *Salinity*, *NOAA Atlas NESDIS 62*, edited by S. Levitus, U.S. Govt. Print. Off., Washington, D. C.

Archer, D., A. Winguth, D. Lea, and N. Mahowald (2000a), What caused the glacial/interglacial atmospheric pCO_2 cycles?, *Rev. Geophys.*, *38*(2), 159–189.

Archer, D. E., G. Eshel, A. Winguth, W. Broecker, R. Pierrehumbert, M. Tobis, and R. Jacob (2000b), Atmospheric pCO_2 sensitivity to the biological pump in the ocean, *Global Biogeochem. Cycles*, *14*(4), 1219–1230.

Bacastow, R. B. (1996), The effect of temperature change of the warm surface waters of the oceans on atmospheric CO_2, *Global Biogeochem. Cycles*, *10*(2), 319–333.

Broecker, W., J. Lynch-Stieglitz, D. Archer, M. Hoffman, E. Maier-Reimer, O. Marchal, T. Stocker, and N. Gruber (1999), How strong is the Harvardton-Bear constraint?, *Global Biogeochem. Cycles*, *13*(4), 817–820.

Bryan, F. (1987), Parameter sensitivity of primitive equation ocean general circulation models, *J. Phys. Oceanogr.*, *17*, 970–985.

Follows, M., R. G. Williams, and J. C. Marshall (1996), The solubility pump of carbon in the subtropical gyre of the North Atlantic, *J. Mar. Res.*, *54*, 605–630.

Follows, M. J., T. Ito, and J. Marotzke (2002), The wind-driven, subtropical gyres and the solubility pump of CO_2, *Global Biogeochem. Cycles*, *16*(4), 1113, doi:10.1029/2001GB001786.

Gebbie, G., and P. Huybers (2006), Meridional circulation during the Last Glacial Maximum explored through a combination of South Atlantic $\delta^{18}O$ observations and a geostrophic inverse model, *Geochem. Geophys. Geosyst.*, *7*, Q11N07, doi:10.1029/2006GC001383.

Gnanadesikan, A. (1999), A simple predictive model for the structure of the oceanic pycnocline, *Science*, *283*, 2077–2079.

Goodwin, P., R. G. Williams, M. J. Follows, and S. Dutkiewicz (2007), Ocean-atmosphere partitioning of anthropogenic carbon dioxide on centennial timescales, *Global Biogeochem. Cycles*, *21*, GB1014, doi:10.1029/2006GB002810.

Goodwin, P., M. J. Follows, and R. G. Williams (2008), Analytical relationships between atmospheric carbon dioxide, carbon emissions, and ocean processes, *Global Biogeochem. Cycles*, *22*, GB3030, doi:10.1029/2008GB003184.

Goodwin, P., R. G. Williams, A. Ridgewell, and M. J. Follows (2009), Climate sensitivity to the carbon cycle modulated by past and future changes in ocean chemistry, *Nat. Geosci.*, *2*, 145–150, doi:10.1028/NGE0416.

Huybers, P., G. Gebbie, and O. Marchal (2007), Can paleoceanographic tracers constrain meridional circulation rates?, *J. Phys. Oceanogr.*, *37*, doi:10.1175/JPO3018.1.

Ito, T., and M. J. Follows (2003), Upper ocean control on the solubility pump of CO_2, *J. Mar. Res.*, *61*, 465–489.

Knox, F., and M. McElroy (1984), Changes in atmospheric CO_2: Influence of biota at high latitudes, *J. Geophys. Res.*, *89*, 4629–4637.

Kwon, E.-Y., and F. Primeau (2006), Optimization and sensitivity study of a biogeochemistry ocean model using an implicit solver and in-situ phosphate data, *Global Biogeochem. Cycles*, *20*, GB4009, doi:10.1029/2005GB002631.

Kwon, E.-Y., and F. Primeau (2008), Optimization and sensitivity study of a global biogeochemistry ocean model using combined in-situ DIC, alkalinity and phosphate data, *J. Geophys. Res.*, *113*, C08011, doi:10.1029/2007JC004520.

Ledwell, J. R., A. J. Watson, and C. S. Law (1993), Evidence for slow mixing across the pycnocline from an open-ocean tracer release experiment, *Nature*, *364*, 701–703.

LeGrand, P., and K. Alverson (2001), Variations in atmospheric CO_2 during glacial cycles from an inverse modeling perspective, *Paleoceanography*, *16*, 604–616.

Locarnini, R. A., A. V. Mishonov, J. I. Antonov, T. P. Boyer, and H. E. Garcia (2006), *World Ocean Atlas 2005*, vol. 1, *Temperature*, *NOAA Atlas NESDIS 63*, edited by S. Levitus, U.S. Govt. Print. Off., Washington, D. C.

Lüthi, D., et al. (2008), High-resolution carbon dioxide concentration record 650,000–800,000 years before present, *Nature*, *453*, 379–382.

Marinov, I., A. Gnanadesikan, J. R. Toggweiler, and J. L. Sarmiento (2006), The Southern Ocean biogeochemical divide, *Nature*, *441*, 964–967.

Marinov, I., M. Follows, A. Gnanadesikan, J. L. Sarmiento, and R. D. Slater (2008a), How does ocean biology affect atmospheric pCO_2? Theory and models, *J. Geophys. Res.*, *113*, C07032, doi:10.1029/2007JC004598.

Marinov, I., A. Gnanadesikan, J. L. Sarmiento, J. R. Toggweiler, M. Follows, and B. K. Mignone (2008b), Impact of ocean circulation on biological carbon storage in the ocean and atmospheric pCO_2, *Global Biogeochem. Cycles*, *22*, GB3007, doi:10.1029/2007GB002958.

Paul, A., and C. Schafer-Neth (2003), Modeling the water masses of the Atlantic Ocean at the Last Glacial Maximum, *Paleoceanography*, *18*(3), 1058, doi:10.1029/2002PA000783.

Petit, J., et al. (1999), Climate and atmospheric history of the past 420,000 years from the Vostok ice core, Antarctica, *Nature*, *399*, 429–436.

Primeau, F. W. (2005), Characterizing transport between the surface mixed layer and the ocean interior with a forward and adjoint global ocean transport model, *J. Phys. Oceanogr.*, *35*(2), 545–564.

Primeau, F. W., and M. Holzer (2006), The ocean's memory of the atmosphere: Residence-time and ventilation-rate distributions of water masses, *J. Phys. Oceanogr.*, *36*, 1439–1456.

Sarmiento, J. L., and R. J. Toggweiler (1984), A new model for the role of the oceans in determining atmospheric pCO_2, *Nature*, *308*, 621–624.

Siegenthaler, U., and T. Wenk (1984), Rapid atmospheric CO_2 variations and ocean circulation, *Nature*, *308*, 624–625.

Siegenthaler, U., et al. (2005), Stable carbon cycle–climate relationship during the Late Pleistocene, *Science*, *310*(5752), 1313–1317.

Sigman, D. M., and E. A. Boyle (2000), Glacial/interglacial variations in atmospheric carbon dioxide, *Nature*, *407*, 859–869.

Toggweiler, J., A. Gnanadesikan, S. Carson, R. Murnane, and J. Sarmiento (2003), Representation of the carbon cycle in box models and GCMs: 1. Solubility pump, *Global Biogeochem. Cycles*, *17*(1), 1026, doi:10.1029/2001GB001401.

Volk, T., and M. I. Hoffert (1985), Ocean carbon pumps: Analysis of relative strengths and efficiencies in ocean-driven atmospheric CO_2 changes, in *The Carbon Cycle and Atmospheric CO_2: Natural Variations Archaen to Present*, *Geophysical Monograph Series*, vol. 32, edited by E. Sundquist and W. Broecker, pp. 99–110, AGU, Washington, D. C.

Wunsch, C. (2003), Determining paleoceanographic circulations, with emphasis on the Last Glacial Maximum, *Quat. Sci. Rev.*, *22*, 371–385.

Zeebe, R. E., and D. Wolf-Gladrow (2001), *CO_2 in Seawater: Equilibrium, Kinetics, Isotopes*, edited by David Halpern, *Elsevier Oceanogr. Ser.*, *65*, 346 pp.

T. DeVries and F. Primeau, Department of Earth System Science, University of California at Irvine, Rowland Hall, Irvine, CA 92697, USA. (tdevries@uci.edu; fprimeau@uci.edu)